Photochemistry Hot Paper

How to cite: *Angew. Chem. Int. Ed.* **2021**, *60*, 11378–11383
International Edition: doi.org/10.1002/anie.202016684
German Edition: doi.org/10.1002/ange.202016684

Optical Manipulation of Subcellular Protein Translocation Using a Photoactivatable Covalent Labeling System

Toshiyuki Kowada, Keisuke Arai, Akimasa Yoshimura, Toshitaka Matsui, Kazuya Kikuchi, and Shin Mizukami**

Abstract: *The photoactivatable chemically induced dimerization (photo-CID) technique for tag-fused proteins is one of the most promising methods for regulating subcellular protein translocations and protein–protein interactions. However, light-induced covalent protein dimerization in living cells has yet to be established, despite its various advantages. Herein, we developed a photoactivatable covalent protein-labeling technology by applying a caged ligand to the BL-tag system, a covalent protein labeling system that uses mutant β-lactamase. We further developed CBHD, a caged protein dimerizer, using caged BL-tag and HaloTag ligands, and achieved light-induced protein translocation from the cytoplasm to subcellular regions. In addition, this covalent photo-CID system enabled quick protein translocation to a laser-illuminated microregion. These results indicate that the covalent photo-CID system will expand the scope of CID applications in the optical manipulation of cellular functions.*

Introduction

Since bioactive molecules such as proteins often exhibit subcellular localization along with other functions, techniques to regulate subcellular protein localization have attracted attention as important tools in cell biology. Recently, a more sophisticated technique that can be used to optically control intracellular protein translocation using optogenetics has been developed.[1] This technique can provide essential information for investigating intracellular protein functions, as microscopic light irradiation helps control protein translocation spatially and temporally to a considerable extent. An alternative approach for regulating subcellular protein localization is chemically induced dimerization (CID) of proteins,[2] which can also be used to manipulate protein–protein interactions in living cells.[3–6] In most cases, the proteins of interest are fused with a tag protein, and a small-molecule dimerizer attaches the two tag ligands on both ends. In addition to optogenetics, a significant effort has been devoted to the development of photoactivatable CID (photo-CID) techniques. In a pioneering study, Schreiber et al. demonstrated the light-control of yeast growth using the light-induced release of rapamycin immobilized on a bead through a photo-cleavable linker.[7] After their study, the caged rapamycin derivatives were used for the photo-regulation of various biomolecular components such as Rho GTPase,[8] kinase,[9] and TEV protease.[10] Recently, an eDHFR-caged trimethoprim system was reported as a suitable non-covalent photo-CID tool,[11] and various chemical biology methods have been studied actively using this system.[12–20]

However, the majority of these photo-CID systems utilize non-covalent protein-labeling technologies to induce protein dimerization. Since covalent CID systems can maintain stable protein dimers regardless of ligand and protein concentrations, the development of a covalent photo-CID system that functions in living cells has been in high demand. Although the light-induced dissociation of protein dimers in living cells has been achieved using a covalent CID system with a photocleavable linker tethering two different tags,[21,22] the light-induced homodimerization of SNAP-tag-fused proteins has only been demonstrated in vitro.[23] Therefore, the optical manipulation of protein localization in living cells by covalent cross-linking using a photo-CID system still requires certain modifications before it can be implemented successfully. In this study, we developed a covalent photo-CID system and demonstrated its application in subcellular protein translocation with high spatiotemporal resolution in living cells.

Results and Discussion

We have previously developed a covalent protein-labeling system, named the BL-tag system, which utilizes a mutant (E166N) TEM-1 β-lactamase (BL-tag) and β-lactam ligands.[24–27] One of the characteristics of the BL-tag system

[*] Dr. T. Kowada, Dr. T. Matsui, Prof. S. Mizukami
Institute of Multidisciplinary Research for Advanced Materials
Tohoku University
Sendai, Miyagi 980-8577 (Japan)
E-mail: shin.mizukami@tohoku.ac.jp
Dr. T. Kowada, K. Arai, Dr. T. Matsui, Prof. S. Mizukami
Graduate School of Life Sciences
Tohoku University
Sendai, Miyagi 980-8577 (Japan)
Dr. A. Yoshimura, Prof. K. Kikuchi
Graduate School of Engineering, Osaka University
2-1 Yamadaoka, Suita, Osaka 565-0871 (Japan)
E-mail: kkikuchi@mls.eng.osaka-u.ac.jp
Prof. K. Kikuchi
Immunology Frontier Research Center
Osaka University
2-1 Yamadaoka, Suita, Osaka 565-0871 (Japan)
and
Center for Quantum Information and Quantum Biology
Osaka University
2-1 Yamadaoka, Suita, Osaka 565-0871 (Japan)
Supporting information and the ORCID identification number(s) for the author(s) of this article can be found under: https://doi.org/10.1002/anie.202016684.

is that various β-lactam antibiotics, such as penicillin and cephalosporin, can be used as specific ligands. The common structure of the ligands contains a carboxylate residue, and the esterification of the carboxylate leads to a reduction in the protein-labeling rate.[28] In addition, the crystal structure of the complex of the mutant E166N β-lactamase and a β-lactam antibiotic suggests that the carboxylate residue plays an important role in complex formation, including the formation of hydrogen bonds.[29] Accordingly, we constructed a photoactivatable covalent protein-labeling system based on the BL-tag system by introducing a bulky photoprotecting group on the carboxy group (Figure 1a). A similar caged β-lactam antibiotic was developed to optically control bacterial growth inhibition.[30] It was assumed that the protected ligand would not be labeled to the BL-tag protein until light-induced deprotection was conducted. To validate this concept, we synthesized two caged derivatives of a fluorescent BL-tag ligand, FPA-DEACM and FPA-DMNPE, having different caging moieties, [7-(diethylamino)coumarin-4-yl)methyl (DEACM) and 1-(4,5-dimethoxy-2-nitrophenyl)ethyl (DMNPE) groups, respectively (Figure 1a). FPA-DEACM was labeled with BL-tag at moderate levels even in dark (unpublished data). Conversely, the labeling of FPA-DMNPE was largely suppressed in the dark, and the specific labeling property was recovered upon UV irradiation in both in vitro and live-cell experiments (Figures 1b–d and S1). The weak fluorescent band in the gel observed under dark conditions was considered to be formed due to slow labeling by FPA-DMNPE, as FPA-DMNPE was not hydrolyzed to FPA in neutral HEPES buffer (Figure S2a). Conversely, FPA was generated at trace levels in 10% FBS-supplemented medium after 2 h of incubation (Figure S2b). Therefore, the faint fluorescence signals obtained in the live-cell imaging with FPA-DMNPE in the absence of UV irradiation could be attributed to the low levels of FPA labeling owing to the hydrolysis of FPA-DMNPE. However, the signals were considerably weak, which led us to conclude that the DMNPE group is a promising photoprotecting group that can be used in the construction of caged BL-tag ligands.

We next designed the caged BL-tag-HaloTag dimerizer (CBHD) (Figure 2a), a photoactivatable chemical dimerizer, for constructing a covalent photo-CID system to link BL-tag with HaloTag, a mutant bacterial haloalkane dehalogenase that specifically forms a covalent bond with a chloroalkane moiety.[31] We assumed that CBHD would initially form a covalent bond with a HaloTag-fused protein, and then form a covalent bond to induce heterodimerization with a BL-tag-fused protein upon UV illumination. CBHD was synthesized according to the process outlined in Scheme S2. HPLC analysis did not reveal hydrolytic conversion from CBHD to BHD in dark for several hours in neutral HEPES buffer or in 10% FBS-supplemented medium (Figure S3). The findings indicate that CBHD is suitable for long-term cellular applications. The photo-conversion of CBHD was investigated under illumination with a Xe lamp at 365 ± 5 nm (Figure 2b). Under UV irradiation, the HPLC peak intensity at 12 min corresponding to CBHD decreased, whereas that at 9.5 min, corresponding to the uncaged dimerizer BHD, increased, in an irradiation time-dependent manner. This efficient photo-uncaging of CBHD was also expected owing to the sufficient absorption at approximately 365 nm (Figure S4). Based on the mass spectrometry (MS) results, the peak formed at 9 min was suggested to result from a derivative of the DMNPE group, and a peak formed at the same retention time was also observed in the uncaging reaction of FPA-DMNPE.

Next, we confirmed the light-induced dimer formation of BL-tag and HaloTag using CBHD in vitro. CBHD (5 μM) was incubated with an N-terminal His-tagged HaloTag (His-Halo, 10 μM) for 30 min for covalent labeling. A maltose-binding protein fused at the C-terminal with BL-tag (MBP-BL, 10 μM) was added to the sample, and the sample was

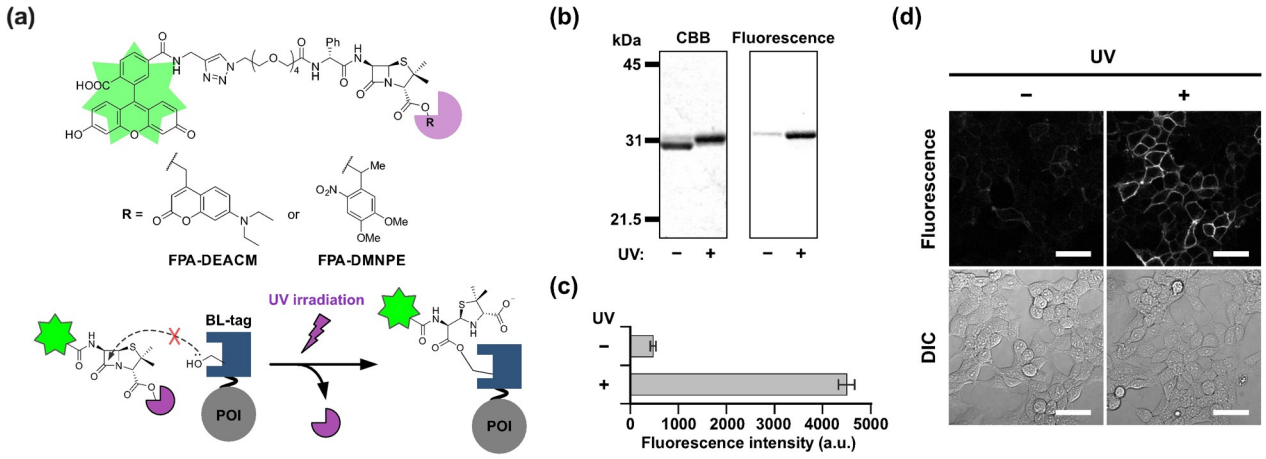

Figure 1. a) Chemical structures of the synthesized caged BL-tag ligands (top), and schematic illustration of light-induced fluorescence labeling of the BL-tag-fused protein (bottom). b) SDS-PAGE analysis of the light-induced labeling reaction of BL-tag with FPA-DMNPE. Coomassie Brilliant Blue (CBB)-stained and fluorescence gel images. [FPA-DMNPE] = 15 μM, [BL-tag] = 10 μM in 100 mM HEPES buffer (pH 7.4). Uncaging light: 365 ± 5 nm, 9.3 mW cm^{-2}, for 5 min at rt. Excitation: 470 nm. Detection: 590 ± 40 nm. c) Fluorescence intensities of the bands corresponding to the labeled BL-tags in the SDS-PAGE analysis shown in (b). The error bars represent s.d. (n = 4). d) Confocal laser scanning microscopy images of BL-tag-fused EGFR (BL-EGFR) labeled with 100 nM FPA-DMNPE. For the condition of UV (+), FPA-DMNPE was uncaged by UV irradiation before probe addition to the live cells. Uncaging light: 365 ± 5 nm, 9.3 mW cm^{-2}, for 5 min at rt. Scale bar: 40 μm.

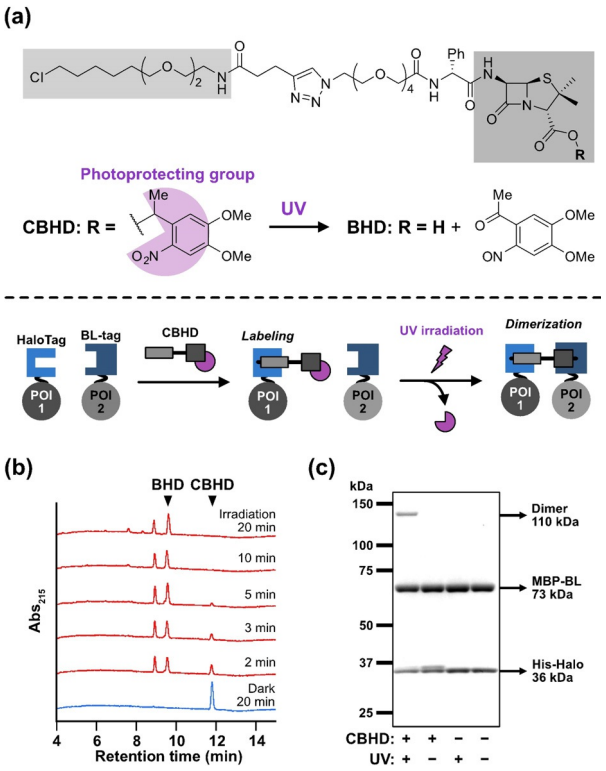

Figure 2. a) Chemical structure of the caged dimerizer, CBHD (top), and schematic illustration of the covalent photo-CID system based on BL-tag and HaloTag (bottom). b) HPLC analysis of the photo-uncaging reaction of CBHD. c) SDS-PAGE analysis of protein dimerization induced by CBHD and UV irradiation. The polyacrylamide gel was stained using CBB. [CBHD] = 5 μM, [His-Halo] = 10 μM, [MBP-BL] = 10 μM in 100 mM HEPES buffer (pH 7.4). Uncaging light: 365 ± 5 nm, 9.6 mW cm^{-2}, for 5 min at rt. Gel: 5%–15% polyacrylamide.

irradiated with UV light for 5 min. After incubation for 60 min, the sample was analyzed using SDS-PAGE (Figure 2c). In the lane loaded with the UV-irradiated sample with CBHD, a new band was observed at approximately 110 kDa corresponding to the dimer of His-Halo (36 kDa) and MBP-BL (73 kDa). Conversely, the lane loaded with the non-UV-irradiated sample did not show a dimer band; however, a new band appeared slightly above the position corresponding to His-Halo, which supposedly corresponded to CBHD-labeled His-Halo (37 kDa). These results demonstrated that the formation of a covalent heterodimer comprising a BL-tag-fused protein and a Halo-Tag-fused protein was induced by UV light irradiation in the presence of CBHD.

We next evaluated intracellular protein translocation as an application of the covalent photo-CID system in live-cell studies (Figure 3a). HEK293T cells were transfected to express both BL-tag-fused EGFP (BL-EGFP) and HaloTag-fused mCherry with a CAAX sequence at the C-terminus (Halo-mCherry-CAAX) targeting the cytosolic interface of the plasma membrane.[32] After the cells were incubated with 10 μM CBHD for 30 min, followed by 30 min incubation in fresh medium for washing out unreacted CBHD, images were acquired using confocal fluorescence microscopy. CBHD formed a covalent bond with membrane-anchored Halo-

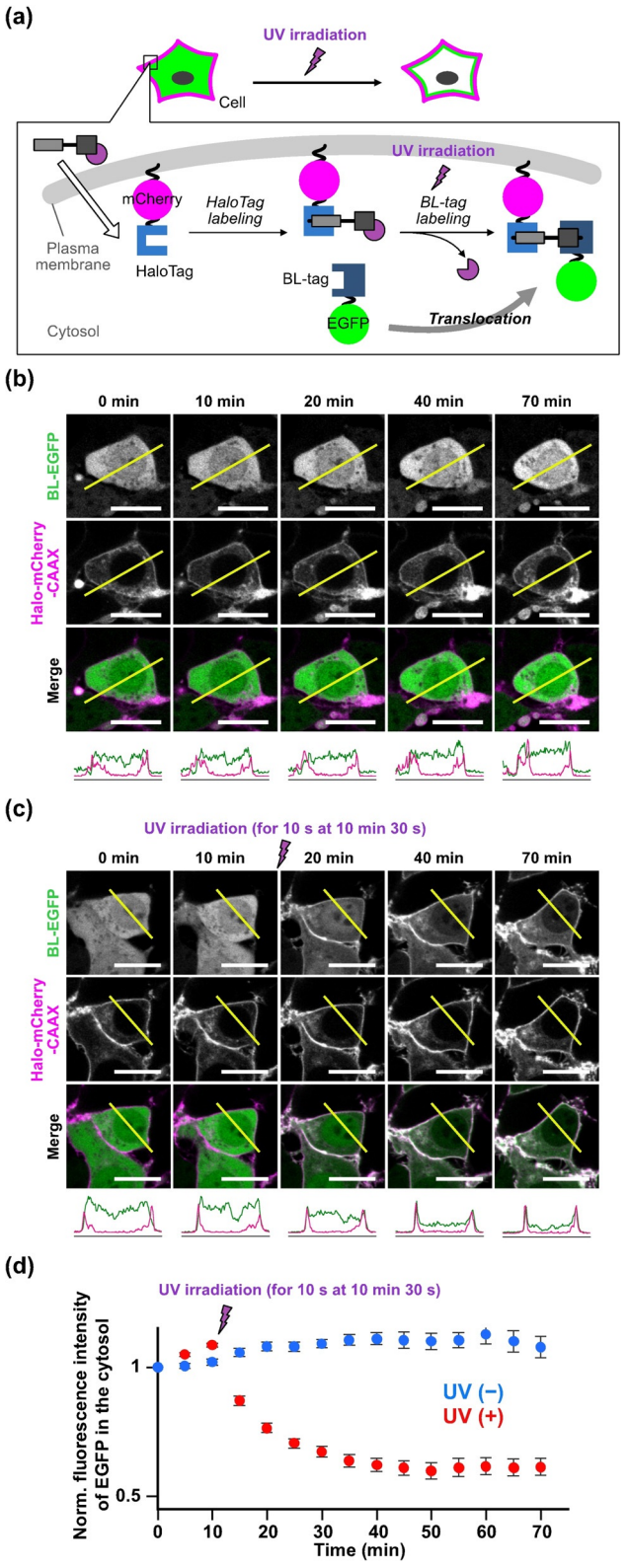

Figure 3. a) Schematic illustration of the photo-CID system using CBHD. b,c) Time-lapse imaging of BL-EGFP translocation to the cytosolic interface of the plasma membrane using CBHD in the absence (b) or presence (c) of UV irradiation. Scale bars: 15 μm. d) Time-course of normalized EGFP fluorescence intensity in the cytosol. The error bars represent the standard error of means (n = 11 (for UV (−)) or 12 cells (for UV (+)) from two independent experiments).

mCherry-CAAX before UV irradiation. Therefore, the green fluorescence signals of BL-EGFP and red fluorescence signals of Halo-mCherry-CAAX were observed from the entire cell and the plasma membrane, respectively, without significant overlap, and no changes were observed in the localization of BL-EGFP for 70 min (Figure 3b). Conversely, UV irradiation for 10 s through the objective lens using an Hg lamp rapidly initiated the translocation of BL-EGFP to the plasma membrane (Figure 3c), which was almost completed approximately within 30 min (Figure 3d). The Pearson correlation coefficient (PCC) changed from 0.39 ± 0.04 to 0.84 ± 0.04 (mean $\pm$ s.e.m., $n = 8$ cells) upon UV irradiation, indicating that most of the BL-EGFP were translocated to the plasma membrane.

To demonstrate the versatility of the covalent photo-CID system, light-induced protein translocation to different subcellular regions was also examined. Halo-mCherry-NLS and Tom20-mCherry-Halo were used instead of Halo-mCherry-CAAX for translocation to the nucleus and mitochondrial outer membrane, respectively, where NLS is a nuclear localization signal from the SV40 large T antigen,[33] and Tom20 is the N-terminal 33 amino acids of the mitochondrial import receptor Tom20.[34] In both cases, light-induced protein translocation was implemented successfully (Figures 4a,b, S5, and S6), as was translocation to the plasma membrane. In addition, the nuclear translocation of BL-EGFP required 50 min (Figure S5), which was longer than the duration required for complete translocation to the plasma membrane (30 min) or the mitochondrial outer membrane (20 min, Figure S6). Possibly, the presence of protein diffusion barriers, such as nuclear pores, delayed the protein translocation process. Colocalization of the two fluorescent proteins was confirmed by calculating the PCCs, 0.42 ± 0.05 (dark) and 0.87 ± 0.02 (UV irradiation) for the nucleus (mean $\pm$ s.e.m., $n = 8$ cells), and 0.53 ± 0.05 (dark) and 0.83 ± 0.02 (UV irradiation) for the mitochondria (mean $\pm$ s.e.m., $n = 8$ cells). When the cells expressing BL-EGFP and Halo-mCherry-NLS were subjected to western blotting analysis, it was confirmed that covalent protein dimerization could be induced by CBHD under whole-sample UV irradiation with a Xe lamp (Figure S7). This application is one of the advantageous properties of the covalent photo-CID system.

Contrary to our expectation, light-triggered protein translocation required several tens of minutes for completion. Although a ten-fold reduction in the concentration of the BL-EGFP-encoding plasmid did not lead to any significant difference in the translocation rates (Figure S8), we believe that the expression levels of both proteins affected the translocation rate; further investigation will be required to confirm this. We also constructed the reverse fusion pair, with BL-EGFP-CAAX expressed in the plasma membrane and Halo-mCherry in the cytosol (Figure S9a). When the cells were transfected with plasmids for BL-EGFP-CAAX and Halo-mCherry in a 1:1 ratio (1250 ng/1250 ng), photo-CID-based translocation was barely observed. However, when the ratio of BL-EGFP-CAAX- and Halo-mCherry-encoding plasmids was altered to 10:1 (909 ng/91 ng), the light-induced translocation of Halo-mCherry from the cytosol to the plasma membrane was clearly observed (Figures S9b,c). In the

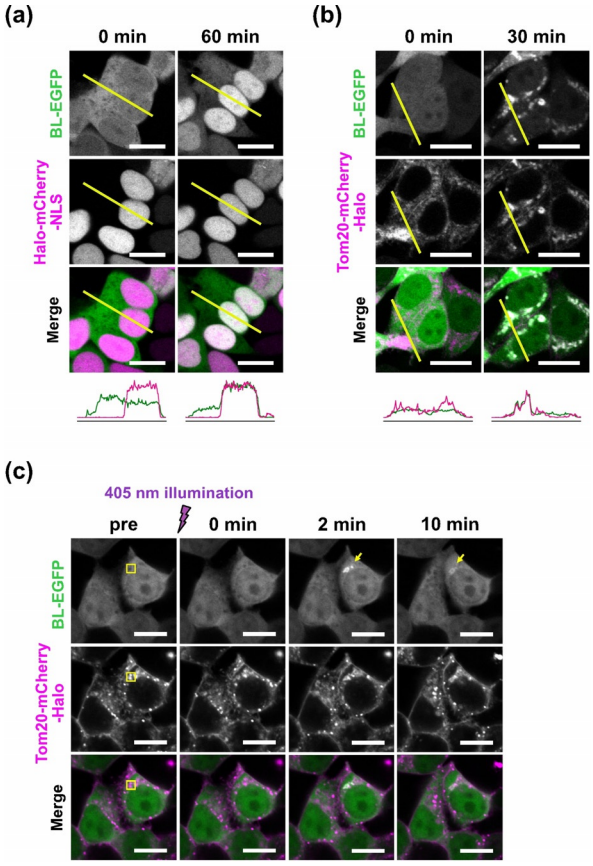

Figure 4. a,b) Light-induced protein (BL-EGFP) translocation to the nucleus (Halo-mCherry-NLS) (a) and mitochondrial outer-membrane (Tom20-mCherry-Halo) (b). Scale bars: 15 μm. c) Laser-induced quick protein (BL-EGFP) translocation to the irradiated microregion (square) in the mitochondrial outer membrane. Scale bar: 10 μm.

experiments performed using this construct pair, the protein translocation was completed within 15 min, although the total concentration of the translocated protein was less than that of the BL-EGFP/Halo-mCherry-CAAX pair (Figure S9d). These results indicate that the kinetics and efficiency of photo-CID-based protein translocation are affected by the anchoring and diffusible proteins selected.

Lastly, to verify the potential of the developed photo-CID system, we attempted subcellular-level light-induced protein translocation. BL-EGFP and Tom20-mCherry-Halo were expressed in the whole-cell area and mitochondrial outer membrane, respectively, and CBHD was labeled to Tom20-mCherry-Halo. After a microregion in a single HEK293T cell was illuminated using a 405 nm laser, EGFP fluorescence signals were rapidly increased in the illuminated region (Figure 4c). This result indicated that photoinduced protein labeling and translocation occur considerably rapidly in the subcellular microregion. The EGFP fluorescence signals in the microregion were restored to levels similar to those in the surrounding regions within 19 min (Figure S10). This could be attributed to the diffusion of the mitochondria in the cell. However, the protein dimer could be retained for a prolonged period in the microregion owing to the fact that the covalent bonds between CBHD and the tag proteins were maintained even at low concentrations. Single-cell-specific light-induced

translocation of Halo-mCherry-NLS was also achieved (Figure S11). Overall, our covalent photo-CID system with CBHD can be applied to subcellular protein dimerization and translocation, and has the potential for local activation of signal transduction pathways at the organelle level.

Conclusion

We developed a photoactivatable covalent protein-labeling system based on our original BL-tag technology by incorporating a photoprotecting DMNPE group into the BL-tag ligand structure. We also used this system to implement photoactivatable protein dimerization using the caged chemical dimerizer CBHD, which covalently links BL-tag and HaloTag. Using this covalent photo-CID system, we achieved the light-induced translocation of cytosolic proteins to various subcellular regions such as the plasma membrane, nucleus, and mitochondrial outer membrane. To our knowledge, this is the first study to achieve light-induced covalent protein dimer formation in living cells. Once a stable covalent bond is formed between the ligand and tag-protein, the resulting protein dimer is maintained stably for a long duration regardless of the ligand–protein complex concentration. This advantageous property of covalent bond formation was also confirmed by the detection of the stable protein dimer in the gel electrophoresis assay. Light-induced subcellular-level protein dimerization has various potential biological applications, such as the sustained activation of ERK in the MAPK signaling pathway[35] in a specific single cell.

Acknowledgements

This work was supported by MEXT KAKENHI Grant Numbers JP18H04605 and JP19H05284, by JSPS KAKENHI Grant Numbers JP17K05921, JP18H02102, JP18F18340, JP19K22241, and JP20K05702, and by the Uehara Memorial Foundation, the Takeda Science Foundation, the Astellas Foundation for Research on Metabolic Disorders, the Tokyo Biochemical Research Foundation, the Kowa Life Science Foundation, the Nakatani Foundation, and the "Dynamic Alliance for Open Innovation Bridging Human, Environment and Materials" Research Program in the "Network Joint Research Center for Materials and Devices". We appreciate the experimental assistance of Hiroto Takahashi, Naoki Honzawa, and Kashfia Ahamed. We thank Tagen Central Analytical Facility for providing the NMR and MS instruments.

Conflict of interest

The authors declare no conflict of interest.

Keywords: caged compound · dimerization · photochemistry · protein–protein interactions · proteins

[1] A. G. Goglia, J. E. Toettcher, *Curr. Opin. Chem. Biol.* **2019**, *48*, 106 – 113.
[2] A. Rutkowska, C. Schultz, *Angew. Chem. Int. Ed.* **2012**, *51*, 8166 – 8176; *Angew. Chem.* **2012**, *124*, 8288 – 8298.
[3] T. Inoue, W. D. Heo, J. S. Grimley, T. J. Wandless, T. Meyer, *Nat. Methods* **2005**, *2*, 415 – 418.
[4] T. Komatsu, I. Kukelyansky, J. M. McCaffery, T. Ueno, L. C. Varela, T. Inoue, *Nat. Methods* **2010**, *7*, 206 – 208.
[5] S. Feng, V. Laketa, F. Stein, A. Rutkowska, A. MacNamara, S. Depner, U. Klingmüller, J. Saez-Rodriguez, C. Schultz, *Angew. Chem. Int. Ed.* **2014**, *53*, 6720 – 6723; *Angew. Chem.* **2014**, *126*, 6838 – 6841.
[6] J. L. Czlapinski, M. W. Schelle, L. W. Miller, S. T. Laughlin, J. J. Kohler, V. W. Cornish, C. R. Bertozzi, *J. Am. Chem. Soc.* **2008**, *130*, 13186 – 13187.
[7] A. Borchardt, S. D. Liberles, S. R. Biggar, G. R. Crabtree, S. L. Schreiber, *Chem. Biol.* **1997**, *4*, 961 – 968.
[8] N. Umeda, T. Ueno, C. Pohlmeyer, T. Nagano, T. Inoue, *J. Am. Chem. Soc.* **2011**, *133*, 12 – 14.
[9] A. V. Karginov, Y. Zou, D. Shirvanyants, P. Kota, N. V. Dokholyan, D. D. Young, K. M. Hahn, A. Deiters, *J. Am. Chem. Soc.* **2011**, *133*, 420 – 423.
[10] K. A. Brown, Y. Zou, D. Shirvanyants, J. Zhang, S. Samanta, P. K. Mantravadi, N. V. Dokholyan, A. Deiters, *Chem. Commun.* **2015**, *51*, 5702 – 5705.
[11] E. R. Ballister, C. Aonbangkhen, A. M. Mayo, M. A. Lampson, D. M. Chenoweth, *Nat. Commun.* **2014**, *5*, 5475.
[12] T. Akera, L. Chmátal, E. Trimm, K. Yang, C. Aonbangkhen, D. M. Chenoweth, C. Janke, R. M. Schultz, M. A. Lampson, *Science* **2017**, *358*, 668 – 672.
[13] C. Aonbangkhen, H. Zhang, D. Z. Wu, M. A. Lampson, D. M. Chenoweth, *J. Am. Chem. Soc.* **2018**, *140*, 11926 – 11930.
[14] E. R. Ballister, S. Ayloo, D. M. Chenoweth, M. A. Lampson, E. L. F. Holzbaur, *Curr. Biol.* **2015**, *25*, R407 – R408.
[15] R. M. Caldwell, J. G. Bermudez, D. Thai, C. Aonbangkhen, B. S. Schuster, T. Courtney, A. Deiters, D. A. Hammer, D. M. Chenoweth, M. C. Good, *Biochemistry* **2018**, *57*, 2590 – 2596.
[16] X. Chen, M. Venkatachalapathy, D. Kamps, S. Weigel, R. Kumar, M. Orlich, R. Garrecht, M. Hirtz, C. M. Niemeyer, Y.-W. Wu, L. Dehmelt, *Angew. Chem. Int. Ed.* **2017**, *56*, 5916 – 5920; *Angew. Chem.* **2017**, *129*, 6010 – 6014.
[17] X. Chen, M. Venkatachalapathy, L. Dehmelt, Y.-W. Wu, *Angew. Chem. Int. Ed.* **2018**, *57*, 11993 – 11997; *Angew. Chem.* **2018**, *130*, 12169 – 12173.
[18] X. Chen, Y.-W. Wu, *Angew. Chem. Int. Ed.* **2018**, *57*, 6796 – 6799; *Angew. Chem.* **2018**, *130*, 6912 – 6915.
[19] D. Ollech, T. Pflästerer, A. Shellard, C. Zambarda, J. P. Spatz, P. Marcq, R. Mayor, R. Wombacher, E. A. Cavalcanti-Adam, *Nat. Commun.* **2020**, *11*, 472.
[20] H. Zhang, C. Aonbangkhen, E. V. Tarasovetc, E. R. Ballister, D. M. Chenoweth, M. A. Lampson, *Nat. Chem. Biol.* **2017**, *13*, 1096 – 1101.
[21] D. Erhart, M. Zimmermann, O. Jacques, M. B. Wittwer, B. Etnst, E. Constable, M. Zvelebil, F. Beaufils, M. P. Wymann, *Chem. Biol.* **2013**, *20*, 549 – 557.
[22] M. Zimmermann, R. Cal, E. Janett, V. Hoffmann, C. G. Bochet, E. Constable, F. Beaufils, M. P. Wymann, *Angew. Chem. Int. Ed.* **2014**, *53*, 4717 – 4720; *Angew. Chem.* **2014**, *126*, 4808 – 4812.
[23] S. Banala, A. Arnold, K. Johnsson, *ChemBioChem* **2008**, *9*, 38 – 41.
[24] S. Mizukami, S. Watanabe, Y. Hori, K. Kikuchi, *J. Am. Chem. Soc.* **2009**, *131*, 5016 – 5017.
[25] S. Mizukami, S. Watanabe, Y. Akimoto, K. Kikuchi, *J. Am. Chem. Soc.* **2012**, *134*, 1623 – 1629.
[26] S. Mizukami, Y. Hori, K. Kikuchi, *Acc. Chem. Res.* **2014**, *47*, 247 – 256.

[27] R. Sato, J. Kozuka, M. Ueda, R. Mishima, Y. Kumagai, A. Yoshimura, M. Minoshima, S. Mizukami, K. Kikuchi, *J. Am. Chem. Soc.* **2017**, *139*, 17397 – 17404.
[28] S. Watanabe, S. Mizukami, Y. Hori, K. Kikuchi, *Bioconjugate Chem.* **2010**, *21*, 2320 – 2326.
[29] N. C. J. Strynadka, H. Adachi, S. E. Jensen, K. Johns, A. Sielecki, C. Betzel, K. Sutoh, M. N. G. James, *Nature* **1992**, *359*, 700 – 705.
[30] W. A. Velema, J. P. van der Berg, W. Szymanski, A. J. M. Driessen, B. L. Feringa, *ACS Chem. Biol.* **2014**, *9*, 1969 – 1974.
[31] G. V. Los, L. P. Encell, M. G. McDougall, D. D. Hartzell, N. Karassina, C. Zimprich, M. G. Wood, R. Learish, R. F. Ohana, M. Urh, D. Simpson, J. Mendez, K. Zimmerman, P. Otto, G. Vidugiris, J. Zhu, A. Darzins, D. H. Klaubert, R. F. Bulleit, K. V. Wood, *ACS Chem. Biol.* **2008**, *3*, 373 – 382.
[32] E. Choy, V. K. Chiu, J. Silletti, M. Feoktistov, T. Morimoto, D. Michaelson, I. E. Ivanov, M. R. Philips, *Cell* **1999**, *98*, 69 – 80.
[33] D. Kalderon, B. L. Roberts, W. D. Richardson, A. E. Smith, *Cell* **1984**, *39*, 499 – 509.
[34] S. Kanaji, J. Iwahashi, Y. Kida, M. Sakaguchi, K. Mihara, *J. Cell. Biol.* **2000**, *151*, 277 – 288.
[35] C. J. Marshall, *Cell* **1995**, *80*, 179 – 185.

Manuscript received: December 16, 2020
Revised manuscript received: February 15, 2021
Accepted manuscript online: February 28, 2021
Version of record online: April 6, 2021

